eXPRESS Polymer Letters Vol.13, No.9 (2019) 785–793
Available online at www.expresspolymlett.com
https://doi.org/10.3144/expresspolymlett.2019.67

Cu^+-containing physically crosslinked chitosan hydrogels with shape memory

Z. Y. Yu[1], Y. Li[1], Z. P. Feng[1], Z. H. Zhang[2], P. Li[1], Y. Chen[1], S. S. Chen[1], P. W. Li[3], Z. M. Yang[3]*

[1]School of Materials Science and Engineering, Beijing Institute of Technology, 100081 Beijing, P. R. China
[2]Beijing Haidian Foreign Language Shi Yan School, 100195 Beijing, China, P. R. China
[3]Agriculture Products Processing Research Institute, Chinese Academy of Tropical Agricultural Sciences, 524001 Zhanjiang, P. R. China

Received 18 January 2019; accepted in revised form 23 April 2019

Abstract. Physically crosslinked chitosan hydrogels have better biocompatibility and possess unique functional characteristics but suffer from poor mechanical properties. In the current study, we prepared Cu^+-containing physically crosslinked chitosan hydrogels by exploiting ammonia fumigation and reduction of Cu^{2+} by $NaHSO_3$. The content of Cu^+ in the prepared hydrogels was in a low range of 4.88–29.27 μmol/g. The mechanical strength of the CTS-Cu^+/NH_3 hydrogels was remarkably improved up to 0.25 MPa and the elongation at break increased with rising content of Cu^+ due to the dynamic crosslinks between chitosan and Cu^+. Moreover, the CTS-Cu^+/NH_3 hydrogels demonstrated evident shape memory after exposure to air by exploiting the different coordination number of Cu^{2+} and Cu^+. Thus, the prepared hydrogels may have good potential applications as biomedical materials.

Keywords: *polymer gels, ammonia fumigation, Cu^+, reduction, shape memory*

1. Introduction

Chitosan is a natural polysaccharide composed of glucosamine and *N*-acetylglucosamine units connected by β-(1,4)-glucoside bonds [1]. Thanks to the presence of plenty of active amino and hydroxyl groups in its structure, chitosan can readily undergo chemical reactions such as alkylation, and has good biocompatibility, biodegradability, and bacteriostatic properties [2]. Hydrogel is a three-dimensional water-retaining material having a similar structure to biological soft tissue [3]. Chitosan hydrogels have a number of advantages and are widely used in medical dressings [4], tissue engineering [5], drug carriers [6], gene therapy, etc. [7].

Chitosan hydrogels can be prepared by chemical crosslinking with the use of a crosslinking agent. Chemically crosslinked hydrogels have good mechanical strength, but the toxicity from residual crosslinking agent (such as glutaraldehyde) seriously reduces the biocompatibility of the hydrogels [8]. By the way, the structure of the chemically crosslinked hydrogels can be hardly controlled. Alternatively, chitosan hydrogels can also be prepared by physical crosslinking via reversible secondary interactions, including electrostatic interactions, metal coordination, hydrogen bonding, hydrophobic interactions, host-guest interactions, etc. [9]. Physical crosslinking not only avoids the use of toxic crosslinking agent but also gives many interesting properties to the chitosan hydrogels, such as self-healing capability [10], injectability [11], temperature sensitivity [12], and response to various stimuli [13]. However, the poor mechanical property of physical crosslinked chitosan hydrogels has limited their application [14].

Physically crosslinked chitosan hydrogels can be prepared by the chelation or electrostatic adsorption

*Corresponding author, e-mail: cylsy@163.com

between the hydroxyl, amino, and *N*-acetylamino groups of chitosan and metal ions containing *d* or *f* unoccupied orbitals [15]. The metal ions can bring various functions to the crosslinked hydrogel, such as antibacterial properties [16], electrochemical sensing [17], specific adsorption, chemical catalysis, etc. [18]. However, the properties of CTS hydrogels complexed with metal ions greatly depend on the process of preparation. Direct complexing of CTS with metal ions was limited by the poor solubility of chitosan in water. Ammonia fumigation is an effective way to cooperate with the process of complexing between chitosan and metal ions [19, 20]. After the amino group of chitosan was protonated in acidic solution, it could keep stably with metal ions in the solution. Upon exposure to ammonia, protonated amino group of chitosan transforms into amino group and forms complex with metal ions resulting in a crosslinking structure. Thus, hydrogels with a uniform structure could be prepared.

The Cu^+ can also be used to coordinate with the amino and hydroxyl groups of polymers. More interestingly, various simple pathways of oxidation could be used to facilitate the conversion between Cu^+ and Cu^{2+}, such as chemical and electrochemical oxidation. Due to the different coordination number of Cu^{2+} and Cu^+, the change in oxidation state is able to adjust the crosslinking density. Thus, compared with the Cu^{2+}-containing hydrogels, mechanical property of Cu^+-containing hydrogels can be readily controlled [21]. Moreover, Cu^+ also performs a unique specificity for binding to cell transporters, which enhances the transport efficiency and therapeutic effects of drugs [22].

In this paper, the acidic solution of chitosan containing $CuCl_2$ was fuminated with ammonia, such that the gradual complexation between $–NH_2$ and Cu^{2+} via the deprotonation of $–NH_3^+$ in ammonia gas could overcome the direct interaction between chitosan and metal ions to avoid defects. The resulting structurally stable chitosan hydrogels containing Cu^{2+} were reduced with $NaHSO_3$ to give the desired uniform and transparent CTS-Cu^+/NH_3 hydrogels. Shape memory was realized in the eventual CTS-Cu^+/NH_3 hydrogels by exploiting the different oxidation states of copper ions.

2. Experimental

2.1. Materials

Chitosan (degree of deacetylation, 90%; average molecular weight, 230 kDa) was purchased from Sinopharm Chemical Reagent Co., Ltd (Shanghai, China). Acetic acid and ammonia were purchased from Xilong Scientific Co., Ltd (Guangdong, China). Copper(II) chloride was purchased from Tianjin Fuchen Chemical Reagent Factory (Tianjin, China). Sodium bisulfite ($NaHSO_3$) was purchased from Beijing Chemical Works (Beijing, China). All chemicals were analytically pure unless indicated otherwise.

2.2. Preparation of CTS-Cu^+/NH_3 hydrogels

To a solution (2.5 wt%, 50 ml) of chitosan in 2.5% v/v acetic acid was added a defined amount of $CuCl_2$ and the mixture was set in a Petri dish and placed in an airtight environment containing 50 ml ammonia. After fumigation for 12 h, the obtained hydrogel was retrieved, washed with distilled water until neutral, then soaked in $NaHSO_3$ (1 mol/l) for 10 min to reduce the Cu^{2+} in the hydrogel to Cu^+, and then washed with distilled water for three times, giving a series of CTS-Cu^+/NH_3 hydrogels that were lyophilized before further analysis. The prepared CTS-Cu^+/NH_3 hydrogels, denoted as CTS0, CTS21, CTS22, CTS23, CTS24, CTS25, CTS26, corresponding to the addition of 0, 4.88, 9.76, 14.64, 19.52, 24.40 and 29.28 μmol/g $CuCl_2$, respectively.

2.3. Characterization by spectroscopy

After freeze drying process, Fourier transform infrared spectrum (FT-IR) was recorded over 750–4000 cm^{-1} on a Nicolet 380 intelligent FT-IR spectrometer (Thermo, United States) with the potassium bromide (KBr) disk technique (6 cm^{-1} resolution, 32 scans). Wide angle X-ray diffraction (XRD) spectrum (2θ = 5–70°) was recorded on a Rigaku D/max-1200 X-ray diffractometer (Rigaku, Tokyo, Japan) at a step length of 0.02° using Ni filter and copper target (λ = 0.15 nm) with 40 mA pipe flow and 40 kV pipe pressure.

2.4. Study on material properties

2.4.1. Mechanical properties

The prepared hydrogels were cut into dumbbell shapes and their mechanical properties were tested on a universal material testing machine (Instron 6022, Instron, USA) at a rate of 100 mm/min to measure the tensile strength (σ) and the elongation at break (ε). Each test was repeated 5 times and the mean value was taken.

2.4.2. Rheological measurements

The rheological properties of the hydrogels were tested at 25 °C on an Anton Paar rheometer (Physica MCR 301, Germany) equipped with parallel plates (25 mm in diameter) at 0.5% strain from sweeping frequency of 0.1 to 700 rad/s to measure the storage modulus (G') and the loss modulus (G'') as a function of angular frequency.

2.4.3. Test of swelling properties

The freeze-dried hydrogel samples (~1 mm thick) were cut into 15 mm×15 mm pieces, weighed and immersed in 50 ml of PBS solution (pH = 7.4) at 25 °C for 3 or 6 h to determine the swelling properties. At the end of immersing, the sample was taken out and wiped with filter papers to completely remove the surface water from the hydrogel and weighed immediately. The swelling ratio was calculated by Equation (1):

$$\text{Swelling ratio} = \frac{W_s - W_d}{W_d} \cdot 100\% \quad (1)$$

where W_s and W_d are the weights of the swollen and dried sample, respectively.

2.4.4. Thermogravimetric test

The freeze-dried hydrogel samples (3–5 mg) were also heated from 50 to 800 °C at 10 °C/min under the protection of 50 ml/min N_2 in a differential thermogravimetric synchronous analyzer (Shimadzu, DTG-60H, Japan).

3. Results and discussion

3.1. Formation of CTS-Cu^+/NH_3 hydrogels

After exposure to ammonia, the transparent and uniform mixture of chitosan solution and $CuCl_2$ gradually formed a gel from the surface to the inside and finally transformed completely into transparent blue hydrogels. As the concentration of Cu^{2+} increased, the color of the hydrogels gradually changed from light blue to dark blue. The hydrogels were then soaked in $NaHSO_3$ to reduce the Cu^{2+}, at which time the color became brown gradually while a good shape of the hydrogel was still maintained (Figure 1a).

Figure 1b schematically shows the formation mechanism of CTS-Cu^+/NH_3 hydrogels. In acidic solution, the $–NH_2$ group of chitosan took the form of $–NH_3^+$, which repelled the positively charged Cu^{2+}. As a result, Cu^{2+} was evenly dispersed into chitosan. Upon exposure of the solution to ammonia, $–NH_3^+$ was gradually neutralized into $–NH_2$ and the lone pair electron in $–NH_2$ slowly coordinated with Cu^{2+}, such that a physically crosslinked network was formed gradually along with the penetration of ammonia from the surface into the hydrogels. The protonated amino groups ($–NH_3^+$) was neutralized incrementally and ensured the formation of uniform and transparent hydrogels, which avoided the defects of precipitation that could be easily generated by the rapid addition of metal ions. Moreover, since the coordination number reduced from 4 (Cu^{2+}) to 2 (Cu^+) [23, 24], the crosslinking density decreased after reduction of Cu^{2+} with $NaHSO_3$, hence soft CTS-Cu^+/NH_3 hydrogels with good shape and transparency were obtained (Figure 1a).

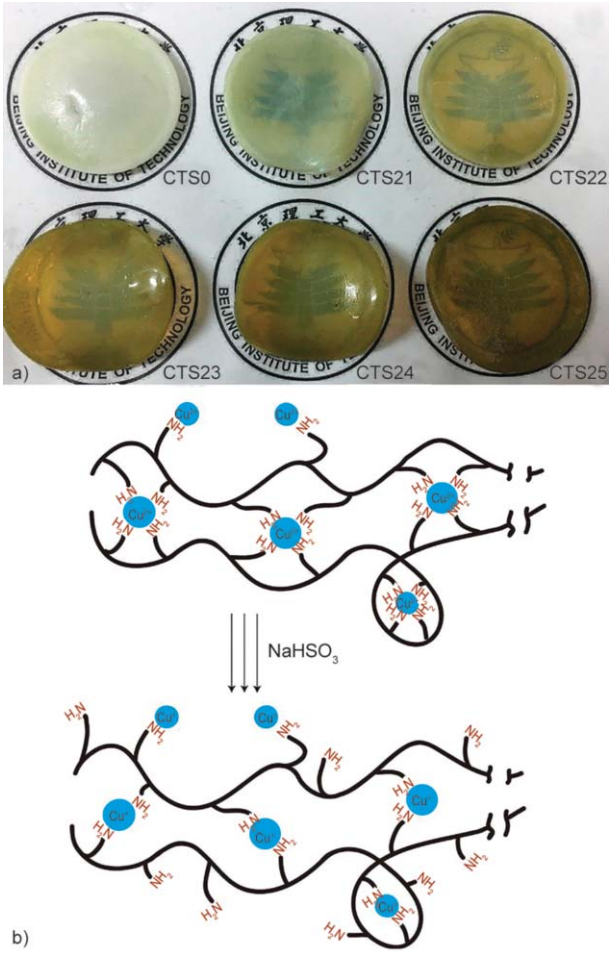

Figure 1. (a) CTS-Cu^+/NH_3 hydrogels with different concentrations of Cu^+; (b) formation mechanism of CTS-Cu^+/NH_3 hydrogels.

3.2. Characterization of spectroscopy

Figure 2 shows the FT-IR spectra of the chitosan hydrogels CTS0, CTS22, and CTS26, in which the wide absorption band at ~3500–3200 cm^{-1} corresponded to the stretching vibration of O–H and N–H.

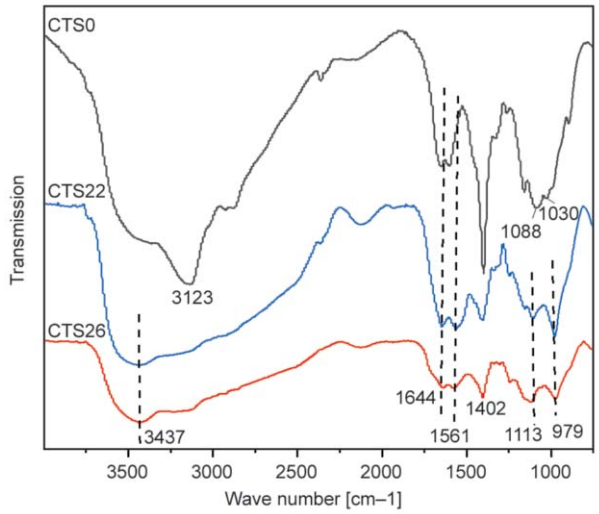

Figure 2. FT-IR spectrum of CTS-Cu^{+}/NH_3 hydrogels.

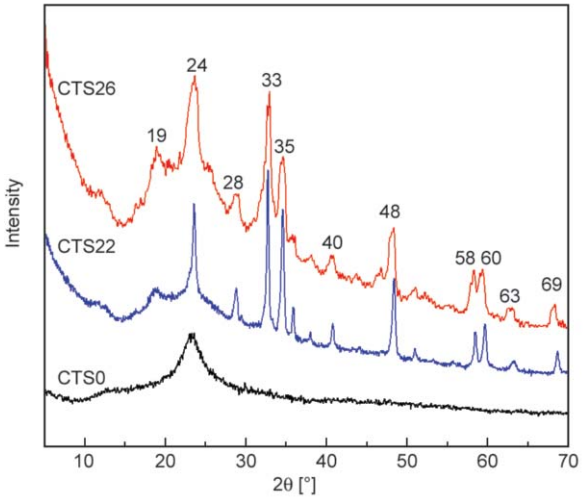

Figure 3. The XRD patterns of CTS-Cu^{+}/NH_3 hydrogels.

The absorption peaks near 1644 and 1599 cm^{-1} were assigned to the stretching vibration of C=O in the amide I band and the bending vibration of amide II band in chitosan, respectively. The peak at 1599 cm^{-1} exhibited a sharp shift to 1561 cm^{-1} due to the complexation between copper ions and $–NH_2$. The absorption peak at 1402 cm^{-1} corresponded to the formed ammonium acetate. The peaks at 1088 and 1030 cm^{-1} bands were attributed to the vibration of secondary and primary hydroxyl of chitosan in CTS0. After the complexation, absorption bands in 1088 cm^{-1} shifted to 1113 cm^{-1} due to the complexation between –OH and copper ions. And the peak at 979 cm^{-1} may be $NaHSO_3$ remained in the network of CTS22 and CTS26. Thus, FTIR successfully demonstrated physical cross-linking between chitosan and copper ions.

Figure 3 shows the XRD patterns of the CTS-Cu^{+}/NH_3 hydrogels. Compared with CTS0, distinct sharp peaks can be observed in Figure 3 due to Cu^{+} and Cu^{2+}. The peaks at 2θ = 19, 28, 33, 40, 58 and 63° were attributed to Cu^{2+} [25, 26]. The diffraction peaks at 2θ = 35, 48, 60 and 69° of CTS21 and CTS26 corresponded to Cu^{+} [27], suggesting that Cu^{2+} was successfully reduced by $NaHSO_3$. And the obvious diffraction peaks at 2θ = 24° were associated with the hydrogen bonding in the hydrogels. As the amount of Cu^{+} increased, the peak at 24° transformed from a wide dispersion peak into a sharp crystallization peak of much higher intensity, which indicated that the addition of Cu^{+} greatly enhanced the hydrogen bonding as well as the crystallinity of the CTS-Cu^{+}/NH_3 hydrogels [28]. Thus XRD results further confirmed the formation of CTS-Cu^{+}/NH_3 hydrogels.

3.3. Mechanical properties

Figure 4 shows the mechanical properties of the CTS-Cu^{+}/NH_3 hydrogels. Although CTS0 was too brittle to be tested, as the amount of Cu^{+} increased, both

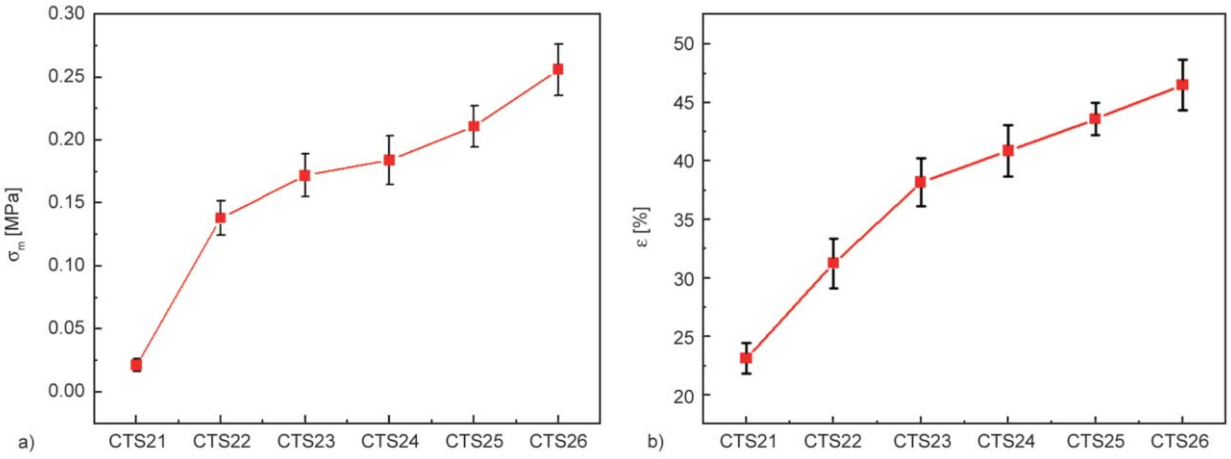

Figure 4. (a) Mechanical strength and (b) elongation at break of the CTS-Cu^{+}/NH_3 hydrogels.

the crosslinking density and the fracture strength of the CTS-Cu^+/NH_3 hydrogels increased gradually. The maximal mechanical strength reached 0.25 MPa for CTS26. The prepared CTS-Cu^+/NH_3 hydrogels had significantly higher mechanical strength than chitosan hydrogels physically crosslinked with polyelectrolytes [29], and were comparable to the CTS/β-glycerophosphate disodium salt hydrogels containing 4% attapulgite [30]. The elongation at break of the CTS-Cu^+/NH3 hydrogels also increased with rising Cu^+ content, indicating that the addition of Cu^+ improved not only the strength but also the toughness, which could be speculated that the physical crosslinking of the chitosan molecular chains with Cu^+ was dynamic, and the chains could slip under external tension. Therefore, both the elongation at break and the mechanical strength of the hydrogels increased with rising Cu^+ content.

3.4. Rheological properties of CTS-Cu^+/NH_3 hydrogels

Figure 5 shows the energy storage modulus (G') and loss modulus (G'') of the CTS-Cu^+/NH_3 hydrogels as a function of angular frequency at 0.5% strain. When the angular frequency was less than 200 rad/s, the G' of all samples was greater than G'', indicating that hydrogels with crosslinked network structure were formed by the coordination of Cu^+ with the $–NH_2$ of chitosan. When the angular frequency exceeded 400 rad/s, it was found that $G' < G''$ for all hydrogels, indicating that the higher shear rate destroyed the crosslinked network structure and the hydrogels changed into viscous liquid, which was the typical characteristic of physical hydrogel. With rising Cu^+ content of the hydrogels, G' gradually decreased and G'' increased firstly and then decreased. Since Cu^+ has a weak ability to accept the lone pair electrons of $–NH_2$ because of its low valence state, the ability of the hydrogels to resist shear force gradually decreased with rising Cu^+ content.

3.5. Swelling properties of CTS-Cu^+/NH_3 hydrogels

The results of swelling ratio test for CTS-Cu^+/NH_3 hydrogels in PBS (pH = 7.4) were shown in Figure 6 and compared with that of CTS0. It could be seen from the figure that the swelling properties of CTS22 was higher than that of CTS0, which indicates that the stable network was formed as complexing of Cu^+ and the capacity for water absorption was increased. However, as increasing of the content of Cu^+, the crosslinking density of the hydrogel was increased and the swelling property of the hydrogels was decreased. As for CTS0, the swelling ratio was sharply decreased as prolonging of the swelling time, which indicates that the above physical crosslinked structure was instable. But for all of the CTS-Cu^+/NH_3 hydrogels, the swelling ratios were slightly increased as prolonging of the swelling time, which means the network structure of CTS-Cu^+/NH_3 hydrogels was more stable and hard to be destroyed.

3.6. Thermogravimetric analysis

Figure 7 shows the TGA and DTG images of the CTS-Cu^+/NH_3 hydrogels, and Table 1 lists the weight loss parameters at different thermogravimetric stages. The thermal weight loss of CTS0 consisted of three stages, corresponding to the loss of binding water, the decomposition of functional groups, and the rupture of the chitosan main chain [31], respectively. The decomposition of CTS0 completed at about 550 °C. The thermal weight loss of the CTS-Cu^+/NH_3 hydrogels

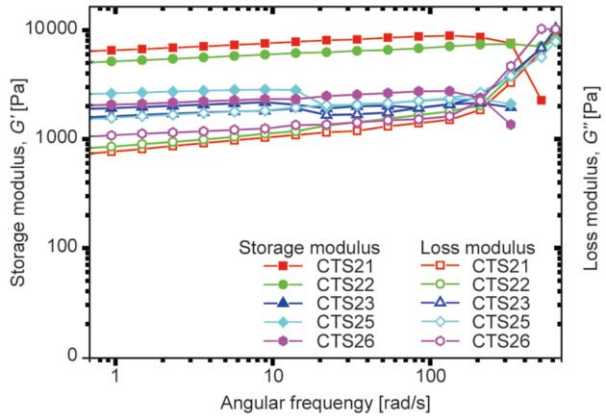

Figure 5. Rheological properties of the CTS-Cu^+/NH_3 hydrogels.

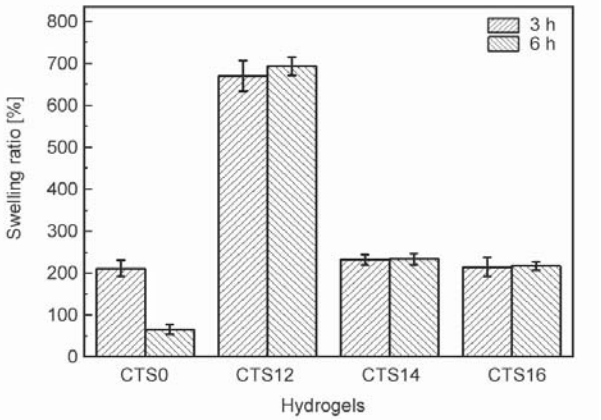

Figure 6. Swelling properties of the CTS-Cu^+/NH_3 hydrogels.

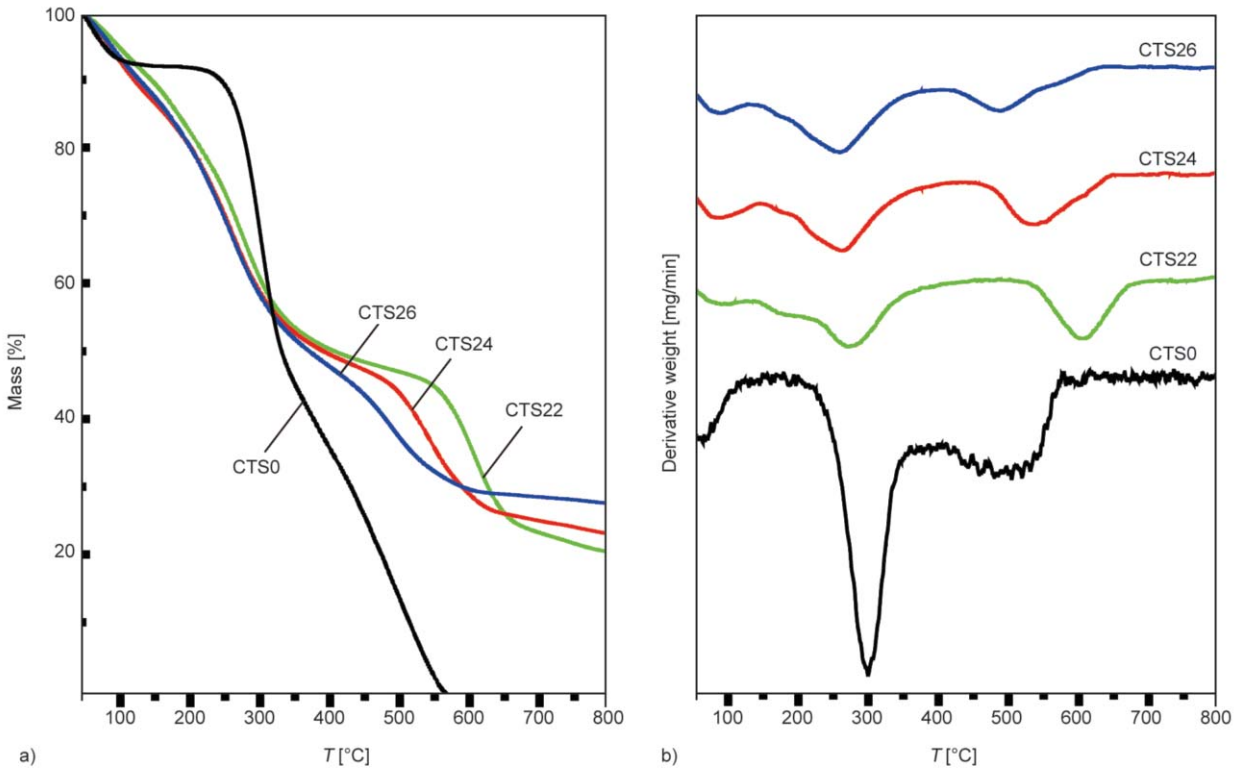

Figure 7. (a) TGA spectra and (b) DTG spectra of the CTS-Cu^+/NH_3 hydrogels.

also consisted of three stages, and the first stage also corresponded to the removal of binding water. Since the crosslink density of the hydrogels was increased as introducing of Cu^+, the amount of binding water in the hydrogels was higher than CTS0. As increasing of the crosslink density for more Cu^+, the weight loss at this stage was decreased. The above results could also be proved by the results of swelling properties. The second stage was attributed to the initial destruction of the physical crosslinking network and the degradation of side groups, and the third stage was attributed to the degradation of chitosan main chain. The CTS-Cu^+/NH_3 hydrogels could not be completely degraded because of the presence of Cu^+, and the weight percentage of the residual hydrogels increased with rising Cu^+ content. Compared with CTS0, low addition of Cu^+ contributed to an increment of decomposition temperature of the third stage and CTS-Cu^+/NH_3 hydrogels exhibited higher thermal stability than CTS0. However, the max weight loss temperature moved from 600 °C (CTS22) to 495 °C (CTS26), which indicated that the increase of copper ion content accelerated the degradation of CTS-Cu^+/NH_3 hydrogels. This observation was consistent with the results reported in literature [31, 32]. And the residual amount of CTS-Cu^+/NH_3 hydrogel was greater than those of CTS0. This might be because that enhanced chelation between Cu^+ and chitosan contributed to an increase in non-volatile components [33, 34].

Table 1. Thermogravimetric parameters of the CTS-Cu^+/NH_3 hydrogels.

Sample	Stage	Temperature range [°C]	Weight loss [%]	Max weight loss temperature [°C]
CTS0	1	45–115	7.331	70
	2	225–345	44.005	300
	3	400–570	35.477	510
CTS22	1	45–140	21.191	80
	2	225–360	25.046	275
	3	360–670	27.760	600
CTS24	1	45–195	18.574	80
	2	195–350	27.821	260
	3	350–650	25.836	540
CTS26	1	50–190	17.631	80
	2	190–340	28.336	260
	3	340–615	22.645	495

3.7. Shape memory performance

Figure 8a shows a cut-out strip of the original CTS-Cu^+/NH_3 hydrogel (i.e., the hydrogel before reduction with $NaHSO_3$). The strip was bent into *U* shape and stood for 48 h in 5 ml deionized water (Figure 8c), and it slowly stretched after it was taken out

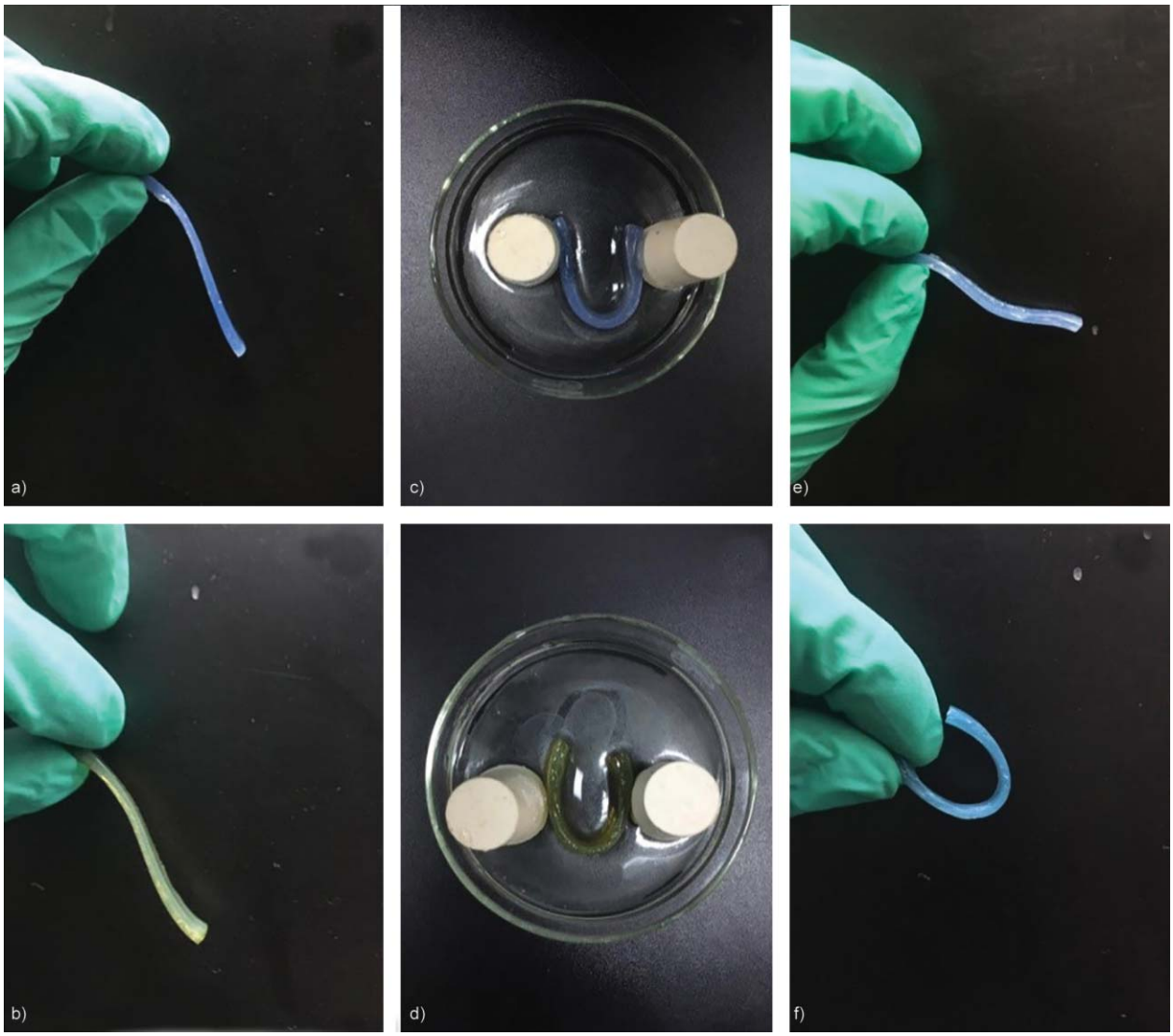

Figure 8. Shape memory of CTS-Cu+/NH3 hydrogels (CTS24). a) and b) were cut-out strips of CTS-Cu^{2+}/NH_3 hydrogels and CTS-Cu^{+}/NH_3 hydrogels, respectively. c) and d) were kept into U shape for 48 h in deionized water. d) and e) were CTS-Cu^{2+}/NH_3 hydrogels and CTS-Cu^{+}/NH_3 hydrogels taken out from deionized water.

(Figure 8e). In contrast, when the strip of the prepared CTS-Cu^{+}/NH_3 hydrogel (CTS24) went through the same procedures (Figure 8b, 8d), the hydrogel strip retained the *U* shape while slowly changing its color from brown to blue (Figure 8f). The Cu^{+} in the CTS-Cu^{+}/NH_3 hydrogels was oxidized in air into Cu^{2+}. Thus, the coordination number of Cu^{+} and Cu^{2+} increased from 2 to 4 and the crosslinking density was enhanced as well as the mechanical strength. As a result, the shape of the bent hydrogel was maintained. And due to the low addition of copper ions, the CTS-Cu^{+}/NH_3 hydrogels may be biocompatible [35], which gives the hydrogels a promising material in tissue engineering, wound dressings, and other fields for this shape memory.

4. Conclusions

In this paper, physically crosslinked chitosan hydrogels carrying Cu^{+} were prepared by complexing Cu^{2+} with chitosan followed by fumigation with ammonia and reduction of Cu^{2+} by $NaHSO_3$. The Cu^{+} content in the above hydrogels was only in a low range of 4.88–29.27 μmol/g, but was able to endow the hydrogels with good mechanical properties. Both the mechanical strength (up to 0.25 MPa) and the elongation at break of the CTS-Cu^{+}/NH_3 hydrogels increased with rising Cu^{+} content. In addition, the CTS-Cu^{+}/NH_3 hydrogels demonstrated evident shape memory and retained the original shape very well after exposure to air. They may thus serve as promising candidates in medical applications.

References

[1] Anitha A., Sowmya S., Kumar P. T. S., Deepthi S., Chennazhi K. P., Ehrlich H., Tsurkan M., Jayakumar R.: Chitin and chitosan in selected biomedical applications. Progress in Polymer Science, **39**, 1644–1667 (2014). https://doi.org/10.1016/j.progpolymsci.2014.02.008

[2] Chen S., Wu G., Zeng H.: Preparation of high antimicrobial activity thiourea chitosan–Ag^{+} complex. Carbohydrate Polymers, **60**, 33–38 (2005). https://doi.org/10.1016/j.carbpol.2004.11.020

[3] Gonçalves A. A. L., Fonseca A. C., Fabela I. G. P., Coelho J. F. J., Serra A. C.: Synthesis and characterization of high performance superabsorbent hydrogels using bis[2-(methacryloyloxy)ethyl] phosphate as crosslinker. Express Polymer Letters, **10**, 248–258 (2016). https://doi.org/10.3144/expresspolymlett.2016.23

[4] Liu H., Wang C., Li. C., Qin Y., Wang Z., Yang F., Li Z., Wang J.: A functional chitosan-based hydrogel as a wound dressing and drug delivery system in the treatment of wound healing. RSC Advances, **8**, 7533–7549 (2018). https://doi.org/10.1039/c7ra13510f

[5] Bush J. R., Liang H., Dickinson M., Botchwey E. A.: Xylan hemicellulose improves chitosan hydrogel for bone tissue regeneration. Polymers for Advanced Technologies, **27**, 1050–1055 (2016). https://doi.org/10.1002/pat.3767

[6] Ali A., Ahmed S.: A review on chitosan and its nanocomposites in drug delivery. International Journal of Biological Macromolecules, **109**, 273–286 (2018). https://doi.org/10.1016/j.ijbiomac.2017.12.078

[7] Kritchenkov A. S., Andranovits S., Skorik Y. A.: Chitosan and its derivatives: Vectors in gene therapy. Russian Chemical Reviews, **86**, 231–239 (2017). https://doi.org/10.1070/Rcr4636

[8] Olaru A-M., Marin L., Morariu S., Pricope G., Pinteala M., Tartau-Mititelu L.: Biocompatible chitosan based hydrogels for potential application in local tumour therapy. Carbohydrate Polymers, **179**, 59–70 (2018). https://doi.org/10.1016/j.carbpol.2017.09.066

[9] Pellá M. C. G., Lima-Tenório M. K., Tenório-Neto E. T., Guilherme M. R., Muniz E. C., Rubira A. F.: Chitosan-based hydrogels: From preparation to biomedical applications. Carbohydrate Polymers, **196**, 233–245 (2018). https://doi.org/10.1016/j.carbpol.2018.05.033

[10] Zhao X., Wu H., Guo B., Dong R., Qiu Y., Ma P.: Antibacterial anti-oxidant electroactive injectable hydrogel as self-healing wound dressing with hemostasis and adhesiveness for cutaneous wound healing. Biomaterials, **122**, 34–47 (2017). https://doi.org/10.1016/j.biomaterials.2017.01.011

[11] Lv X., Liu Y., Song S., Tong C., Shi X., Zhao Y., Zhang J., Hou M.: Influence of chitosan oligosaccharide on the gelling and wound healing properties of injectable hydrogels based on carboxymethyl chitosan/alginate polyelectrolyte complexes. Carbohydrate Polymers, **205**, 312–321 (2019). https://doi.org/10.1016/j.carbpol.2018.10.067

[12] Zhang W., Jin X., Li H., Zhang R-R., Wu C-W.: Injectable and body temperature sensitive hydrogels based on chitosan and hyaluronic acid for pH sensitive drug release. Carbohydrate Polymers, **186**, 82–90 (2018). https://doi.org/10.1016/j.carbpol.2018.01.008

[13] Sun Z. F., Lv F. C., Cao L. J., Liu L., Zhang Y., Lu Z. G.: Multistimuli-responsive, moldable supramolecular hydrogels cross-linked by ultrafast complexation of metal ions and biopolymers. Angewandte Chemie, International Edition, **54**, 7944–7948 (2015). https://doi.org/10.1002/anie.201502228

[14] Montembault A., Viton C., Domard A.: Rheometric study of the gelation of chitosan in aqueous solution without cross-linking agent. Biomacromolecules, **6**, 653–662 (2005). https://doi.org/10.1021/bm049593m

[15] Guibal E.: Interactions of metal ions with chitosan-based sorbents: A review. Separation and Purification Technology, **38**, 43–74 (2004). https://doi.org/10.1016/j.seppur.2003.10.004

[16] Wahid F., Wang H-S., Zhong C., Chu L-Q.: Facile fabrication of moldable antibacterial carboxymethyl chitosan supramolecular hydrogels cross-linked by metal ions complexation. Carbohydrate Polymers, **165**, 455–461 (2017). https://doi.org/10.1016/j.carbpol.2017.02.085

[17] Fu L., Wang A., Lyv F., Lai G., Zhang H., Yu J., Lin C-T., Yu A., Su W.: Electrochemical antioxidant screening based on a chitosan hydrogel. Bioelectrochemistry, **121**, 7–10 (2018). https://doi.org/10.1016/j.bioelechem.2017.12.013

[18] Guibal E., Vincent T., Navarro R.: Metal ion biosorption on chitosan for the synthesis of advanced materials. Journal of Materials Science, **49**, 5505–5518 (2014). https://doi.org/10.1007/s10853-014-8301-5

[19] Rogina A., Lončarević A., Antunović M., Marijanović I., Ivanković M., Ivanković H.: Tuning physicochemical and biological properties of chitosan through complexation with transition metal ions. International Journal of Biological Macromolecules, **129**, 645–652 (2019). https://doi.org/10.1016/j.ijbiomac.2019.02.075

[20] Li P., Zhao J., Chen Y., Cheng B., Yu Z., Zhao Y., Yan X., Tong Z., Jin S.: Preparation and characterization of chitosan physical hydrogels with enhanced mechanical and antibacterial properties. Carbohydrate Polymers, **157**, 1383–1392 (2016). https://doi.org/10.1016/j.carbpol.2016.11.016

[21] Harris R. D., Auletta J. T., Motlagh S. A. M., Lawless M. J., Perri N. M., Saxena S., Weiland L. M., Waldeck D. H., Clark W. W., Meyer T. Y.: Chemical and electrochemical manipulation of mechanical properties in stimuli-responsive copper-cross-linked hydrogels. Acs Macro Letters, **2**, 1095–1099 (2014). https://doi.org/10.1021/mz4004997

[22] Xi Z., Guo W., Tian C., Wang F., Liu Y.: Copper binding promotes the interaction of cisplatin with human copper chaperone Atox1. Chemical Communications, **49**, 11197–11199 (2013). https://doi.org/10.1039/c3cc45905e

[23] Martina K., Leonhardt S. E. S., Ondruschka B., Curini M., Binello A., Cravotto G.: *In situ* cross-linked chitosan Cu(I) or Pd(II) complexes as a versatile, eco-friendly recyclable solid catalyst. Journal of Molecular Catalysis A: Chemical, **334**, 60–64 (2011). https://doi.org/10.1016/j.molcata.2010.10.024

[24] Huang Y., Huang J., Cai J., Lin W., Lin Q., Wu F., Luo J.: Carboxymethyl chitosan/clay nanocomposites and their copper complexes: Fabrication and property. Carbohydrate Polymers, **134**, 390–397 (2015). https://doi.org/10.1016/j.carbpol.2015.07.089

[25] Park E. D., Lee J. S.: Effects of copper phase on co oxidation over supported wacker-type catalysts. Journal of Catalysis, **180**, 123–131 (1998). https://doi.org/10.1006/jcat.1998.2263

[26] Sun Q., Yang Y., Zhao Z., Zhang Q., Zhao X., Nie G., Jiao T., Peng Q.: Elaborate design of polymeric nanocomposites with Mg(II)-buffering nanochannels for highly efficient and selective removal of heavy metals from water: Case study for Cu(II). Environmental Science: Nano, **5**, 2440–2451 (2018). https://doi.org/10.1039/C8EN00611C

[27] Zhang F., Lai J., Huang Y., Li F., Luo G., Chu G.: A green method for preparing CuCl nanocrystal in deep eutectic solvent. Australian Journal of Chemistry, **66**, 237–240 (2013). https://doi.org/10.1071/Ch12387

[28] Ma G., Qian B., Yang J., Hu C., Nie J.: Synthesis and properties of photosensitive chitosan derivatives. International Journal of Biological Macromolecules, **46**, 558–561 (2010). https://doi.org/10.1016/j.ijbiomac.2010.02.009

[29] Yu C., Yu L., Yiguli A., Yanwei Z., Yi D., Yanwen G., Yanchun Y., Huimin T.: Structure and drug release of superabsorbent sponge prepared by polyelectrolyte complexation and freezing-induced phase separation. Journal of Applied Polymer Science, **126**, 1307–1315 (2012). https://doi.org/10.1002/app.36937

[30] Wang Q., Chen D.: Synthesis and characterization of a chitosan based nanocomposite injectable hydrogel. Carbohydrate Polymers, **136**, 1228–1237 (2016). https://doi.org/10.1016/j.carbpol.2015.10.040

[31] Baran T., Menteş A., Arslan H.: Synthesis and characterization of water soluble O-carboxymethyl chitosan schiff bases and Cu(II) complexes. International Journal of Biological Macromolecules, **72**, 94–103 (2015). https://doi.org/10.1016/j.ijbiomac.2014.07.029

[32] Liu Y., Chen Y., Zhao Y., Tong Z., Chen S.: Superabsorbent sponge and membrane prepared by polyelectrolyte complexation of carboxymethyl cellulose/hydroxyethyl cellulose-Al^{3+}. Bioresources, **10**, 6479–6495 (2015).

[33] Baran T., Menteş A.: Cu(II) and Pd(II) complexes of water soluble O-carboxymethyl chitosan schiff bases: Synthesis, characterization. International Journal of Biological Macromolecules, **79**, 542–554 (2015). https://doi.org/10.1016/j.ijbiomac.2015.05.021

[34] Zhou J., Gao F., Jiao T., Xing R., Zhang L., Zhang Q., Peng Q.: Selective Cu(II) ion removal from wastewater via surface charged self-assembled polystyrene-schiff base nanocomposites. Colloids and Surfaces A: Physicochemical and Engineering Aspects, **545**, 60–67 (2018). https://doi.org/10.1016/j.colsurfa.2018.02.048

[35] Saporito-Magriñá C. M., Musacco-Sebio R. N., Andrieux G., Kook L., Orrego M. T., Tuttolomondo M. V., Desimone M. F., Boerries M., Borner C., Repetto M. G.: Copper-induced cell death and the protective role of glutathione: The implication of impaired protein folding rather than oxidative stress. Metallomics, **10**, 1743–1754 (2018). https://doi.org/10.1039/C8MT00182K